Journal of Physiology (1991), **435**, *pp.* 349–372
With 10 figures
Printed in Great Britain

TOTAL AND FREE MYOPLASMIC CALCIUM DURING A CONTRACTION CYCLE: X-RAY MICROANALYSIS IN GUINEA-PIG VENTRICULAR MYOCYTES

BY MARIA FIORA WENDT-GALLITELLI AND GERRIT ISENBERG

From the Department of Physiology II, University of Tübingen and Department of Physiology, University of Cologne, Köln, Germany

(*Received 9 April 1990*)

SUMMARY

1. At 36 °C and 2 mM $[Ca^{2+}]_o$ single guinea-pig ventricular myocytes were voltage clamped with patch electrodes. With a paired-pulse protocol applied at 1 Hz, a first pulse to +5 mV was followed by a second pulse to +50 mV. When paired pulsing had potentiated the contraction to the maximum, the cells were shock-frozen for electron-probe microanalysis (EPMA). Shock-freezing was timed at the end of diastole (−80 mV) or at different times during systole (+5 mV).

2. The same paired-pulse protocol was applied to another group of myocytes from which contraction and $[Ca^{2+}]_i$ was estimated by microfluospectroscopy (50 μM-Na_5-Indo-1). Potentiation moderately reduced diastolic sarcomere length from 1·85 to 1·82 μm and increased diastolic $[Ca^{2+}]_i$ from about 95 to 180 nM. In potentiated cells, during the first pulse, contraction peaked within 128 ± 25 ms after start of depolarization. $[Ca^{2+}]_i$ peaked within 25 ms to 890 ± 220 nM (mean ± S.E.M.) and fell within 100 ms to about 450 nM.

3. ΣCa_{myo}, the total calcium concentration in the overlapping myofilaments (A-band), was measured by EPMA in seventeen potentiated myocytes. During diastole, ΣCa_{myo} was 2·6 ± 0·4 mmol (kg dry weight (DW))$^{-1}$ which can be converted to 0·65 mM (mmoles per litre myofibrillar space). Since $[Ca^{2+}]_i$ was 180 nM, we estimate that 99·97 % of total calcium is bound.

4. A time course for systolic ΣCa_{myo} was determined by shock-freezing thirteen cells at different times after start of depolarization to +5 mV. ΣCa_{myo} was 5·5 ± 0·3 mmol (kg DW)$^{-1}$ (1·4 mM) after 15–25 ms, 4·6 ± 0·5 mmol (kg DW)$^{-1}$ (1·1 mM) after 30–45 ms, and 3·1 mmol (kg DW)$^{-1}$ (0·8 mM) after 60–120 ms. The fast time course of ΣCa_{myo} suggests that calcium binds to and unbinds from troponin C at a fast rate. Hence, it is the slow kinetics of the cross-bridges that determines the 130 ms time-to-peak shortening.

5. Mitochondria of potentiated cells contained during diastole a total calcium concentration, ΣCa_{mito}, of 1·3 ± 0·2 mmol (kg DW)$^{-1}$ (0·4 mM). During the initial 15–25 ms of systole, ΣCa_{mito} did not change, however, during 30–45 ms ΣCa_{mito} rose to 3·7 ± 0·5 mmol (kg DW)$^{-1}$ (1·2 mM). The data suggest that ΣCa_{mito} can follow ΣCa_{myo} with some delay, thereby participating in both slow diastolic and fast systolic changes in total calcium (ΣCa), at least under the given conditions.

MS 8411

6. Junctional and corbular sarcoplasmic reticulum (SR) at the level of the Z-line had a diastolic total calcium concentration, ΣCa_{SR}, of $8{\cdot}7 \pm 1{\cdot}3$ mmol (kg DW)$^{-1}$ (2·4 mM), significantly higher than ΣCa_{myo}. Twenty milliseconds after the beginning of depolarization ΣCa_{SR} had fallen to $4{\cdot}1 \pm 0{\cdot}4$ mmol (kg DW)$^{-1}$ (1·1 mM), during the following systole ΣCa_{SR} recovered. The difference between ΣCa_{SR} and ΣCa_{myo} has the property expected of a 'Ca-release compartment'.

7. Our data indicate for the myofibrillar space a Ca^{2+}-buffering capacitance of 1·5 mmol ΣCa_{myo} per pCa unit between pCa 7 and 6. The concentration of troponin C is insufficient to account for this value. To present a model explaining the results requires the assumption of additional Ca^{2+}-binding sites. The effect of potentiation on diastolic $[Ca^{2+}]_i$ and ΣCa_{myo} requires a postulation of 600 μM additional Ca^{2+}, Mg^{2+} sites and the rapid systolic transients require the assumption of 2000 μM additional 'fast' Ca^{2+}-binding sites.

INTRODUCTION

In this paper, we report measurements of total myofibrillar calcium concentration as it changes during the contraction–relaxation cycle of a heart ventricular myocyte. The measurements were made by means of electron-probe microanalysis (EPMA). EPMA measures the sum of ionized $[Ca^{2+}]_i$ and bound calcium, this 'total calcium' is symbolized here with 'ΣCa'. EPMA can measure ΣCa in those intracellular compartments as the myofibrillar space of the A-band (ΣCa_{myo}), the mitochondria (ΣCa_{mito}) or the sarcoplasmic reticulum (ΣCa_{SR}). The concentrations were measured on the basis of the dry mass of the analysed volume (mmol (kg dry weight (DW))$^{-1}$), and they can be converted into molarity (mmoles per litre compartment, mM) or molality (mmoles per kilogram water in the compartment) for comparison. Here, the time course of ΣCa_{myo} will be compared with the one of free $[Ca^{2+}]_i$ as it is measured by the fluorescence Ca^{2+} indicator Indo-1, as well as with the time course of contraction (unloaded shortening).

The method was applied to ventricular myocytes, at 36 °C and at an extracellular calcium concentration of 2 mM. At 1 Hz, the cells were stimulated with paired voltage clamp pulses. A first pulse to +5 mV controlled, via the membrane potential, the calcium current I_{Ca} that induces release of Ca^{2+} from the sarcoplasmic reticulum (SR) leading to contraction. A second pulse activated Ca^{2+} influx through the Na^+–Ca^{2+} exchanger and potentiated contractions to an optimum. For this potentiated state, ΣCa was analysed in either diastole or at different times of systole, ΣCa of the compartments being preserved by cryotechniques. For the 'time course' of ΣCa during the contraction–relaxation cycle, a large number of experiments was necessary: the selected moment of shock-freezing ends the experiment, and a new experiment with another cell is required to obtain the next time point. Due to cell-to-cell variability, for each time point data from several cells must be averaged. The experimental effort seems to be justified by the new result that the total calcium concentration in the myofibrillar space increases during systole by millimolar amounts, and that this change occurs and dissipates within approximately 100 ms.

Parts of this work have been presented in abstract form (Wendt-Gallitelli & Isenberg, 1990).

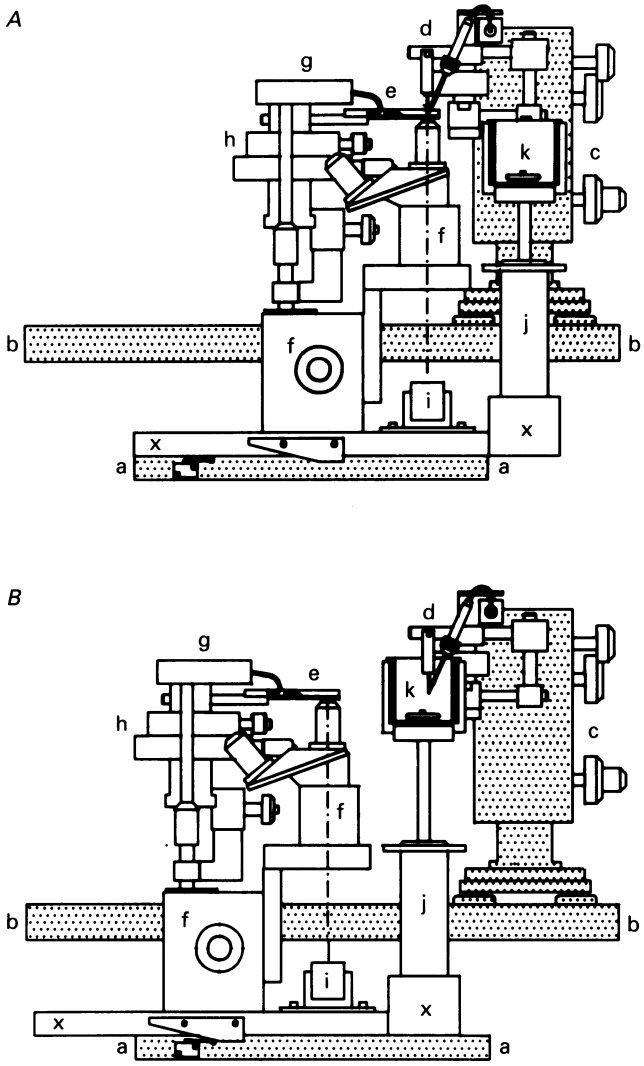

Fig. 1. Device for shock-freezing of voltage clamped ventricular myocytes, shown before (*A*) and after (*B*) shock-freezing. The two plates (a) and (b) are fixed independently to prevent transfer of vibrations from the moving parts to the electrode. Plate b supports a Leitz micromanipulator (c) that bears the silver holder (d), and a hydraulic Narashige micromanipulator for the electrode at the head stage of the amplifier. Parts b, c and d are kept still during the shock-freezing. The sliding stage x supports a simple microcope (f) adapted through a prism (i) to a TV camera (not shown). x also supports, via the manipulator (h), the experimental chamber (e) into which solution flows from the heat exchanger (g). During shock-freezing, the sliding stage (x) is moved backwards by means of pneumatic pistons. When the sliding stage x has positioned the silver holder, cell and electrode into the air above the beaker with the coolant (k), the beaker is pushed upwards with the piston (j).

METHODS

Myocyte isolation procedure. Ventricular myocytes were isolated according to Bendukidze, Isenberg & Klöckner (1985). During the initial 5 min, the heart was retrogradely perfused (36 °C) with a calcium-free 'cell medium' (120 mM-NaCl, 12 mM-KCl, 1·2 mM-$MgCl_2$, 20 mM-glucose, 20 mM-taurine, 5 mM-sodium pyruvate, 10 mM-HEPES/NaOH, pH 7·3). This was followed by a 7 min perfusion with the same medium but supplemented with 50 mg l^{-1} protease (pronase type E, Serva, Germany) and 250 μM-$CaCl_2$. The left ventricle was chopped into chunks that were stirred in the same enzyme-containing medium for three periods of 10 min each. The released myocytes were suspended in cell medium containing 0·5 mM-$CaCl_2$ and stored at 22 °C until used. For the experiment, a drop of cell medium was pipetted into a 0·1 ml chamber. When the cells had settled to the bottom of the chamber, they were continuously superfused (36 °C) with a physiological salt solution (PSS: 150 mM-NaCl, 5·4 mM-KCl, 2 mM-$CaCl_2$, 1·2 mM-$MgCl_2$, 5 mM-glucose, 5 mM-HEPES/NaOH, pH 7·4).

Voltage clamp experiments were performed according to the whole-cell configuration of the patch clamp technique. Pipettes were pulled from borosilicate glass capillaries of 2 mm outer diameter to tips of about 2 μm (tip resistance 1·5 MΩ). The pipettes were filled with an 'electrode solution' composed to 140 mM-KCl, 5 mM-Na_2ATP, 5·5 mM-$MgCl_2$, 20 μM-EGTA, 10 mM-HEPES/KOH (pH 7·4).

Contractile force (Fig. 6) was measured as described recently (Shepherd, Vornanen & Isenberg, 1990). Briefly, the isolated myocyte was attached by poly-L-lysine to the bevelled ends of a pair of thin glass rods having a compliance of 0·76 m N^{-1}. The contraction caused a 1 μm displacement of the rods, the motion of which was converted to an output voltage by phototransistors placed in the microscope. The same device could be used for recording the shortening of the unloaded myocyte (Fig. 10). Off-line, the averaged sarcomere length was estimated from TV tape-recordings (Isenberg, 1982).

Measurements of $[Ca^{2+}]_i$ were carried out with the ratio technique of Indo-1 fluorescence (Grynkiewicz, Poenie & Tsien, 1985). Details of the set-up and the calibration were described recently (Ganitkevich & Isenberg, 1991). Briefly, a Zeiss IM-35 microscope was used for epifluorescence and for conventional through-light microscopy (600 nm). Indo-1 (50 μM; Boehringer, Mannheim, Germany) was added to the electrode solution from which it diffused into the myoplasm. A 30 μm wide part of the myocyte was illuminated at 360 nm through an UV-passing objective (Nikon, 100-fold oil immersion). The fluorescent light was subsequently split by interference filters (Schott, Mainz, Germany) to pass wavelength bands of 410 ± 15 and 490 ± 15 nm to two photomultipliers (DuBell & Houser, 1989). Background fluorescence was measured at both wavelengths just prior to rupturing the membrane patch and analog subtracted. After rupturing the patch, dye loading of the cell usually reached a steady state of about 100 times background after 1–2 min. Data was processed through a CED-1401 interface (Cambridge Electronics, UK) and an IBM-compatible PC as a host. Simultaneously, on-line processing was performed with an analog circuit to a pen writer. Intracellular calibration of the $[Ca^{2+}]_i$ signals revealed for the apparatus a constant ($K_D B$ value) of 862 nM (Ganitkevich & Isenberg, 1991). Calibration seems to be subject to uncertainty because the fluorescent probe probably binds to constituents of the cytosol thereby changing the affinity and kinetics of calcium binding (Baylor & Hollingworth, 1988). Hence, our $[Ca^{2+}]_i$ measurements may be erroneous by a factor of 2. Results are expressed as means $\pm$ S.E.M., and each figure is representative for at least three similar experiments.

Shock-freezing of the myocyte. A myocyte with clear cross-striations was sucked on to the patch electrode, lifted from the bottom of the chamber and transferred into the funnel of the silver holder where it was placed on a thin film of Pioloform (details in Wendt-Gallitelli & Isenberg, 1989). After the patch of membrane was ruptured, the resting potentials were -85 mV; the action potentials had an amplitude of 134 ± 5 mV and a duration of 220 ± 38 ms. Then, the voltage clamp was switched on. (For the pulse protocol see bottom panel of Fig. 2.) Potentiation of contraction was achieved with at least ten paired clamp pulses. Then, a series of computer-controlled pneumatic movements was initiated (details in Wendt-Gallitelli & Isenberg, 1989). The microscope with the chamber was slid backwards, this movement positioned the silver holder with the myocyte, the PSS and the electrode in the air over a container. Finally, this container was pneumatically pushed upward for 'shock-freezing' the myocyte with supercooled propane (-196 °C). The mechanical movements did not damage the myocyte or induce leakage across the cell membrane. Integrity of

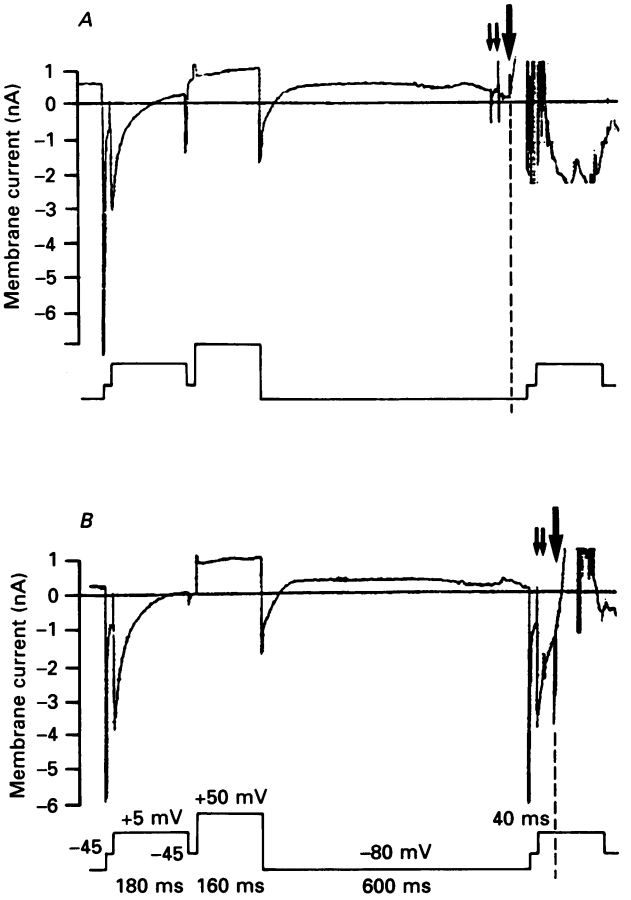

Fig. 2. The membrane current can be used as a protocol to monitor the events during shock-freezing. *A*, shock-freezing at the end of diastole. *B*, shock-freezing during systole, 40 ms after start of depolarization to +5 mV. The panels show the membrane current in response to the voltage clamp protocol (lower traces). During diastole, the holding potential is −80 mV. At a rate of 1 Hz, paired voltage clamp pulses are applied. The first pulse starts with a short 20 ms depolarization to −45 mV that activates and inactivates a TTX-sensitive Na^+ current (peak off scale). Next, a 180 ms pulse to +5 mV activates and inactivates an inward calcium current I_{Ca}. After a short 20 ms repolarization to −45 mV, the second pulse depolarizes the membrane to +50 mV for 160 ms and induces an outward current carried mostly by K^+ ions. The final repolarization to −80 mV induces a large inward tail current due to electrogenic Na^+–Ca^{2+} exchange. When the cell in the holder is moved out of the experimental chamber and into the air, no change in membrane current is seen. Two small capacitive artifacts (paired small arrows) reflect the operation of the magnetic valve controlling the vertical movement of the piston. Contact with the −196 °C coolant (large arrow, dashed line) is indicated by a large capacitive artifact followed by a large outward current.

the sarcolemmal membrane was monitored by continuously recording the membrane current until the very moment of shock-freezing (Fig. 2).

Timing. The pneumatic movements were under the control of the computer. However, due to the large mass that had to be accelerated, there was 5 ms scattering of the actual moment of shock-freezing around the programmed value. The final events of shock-freezing produced signals in the

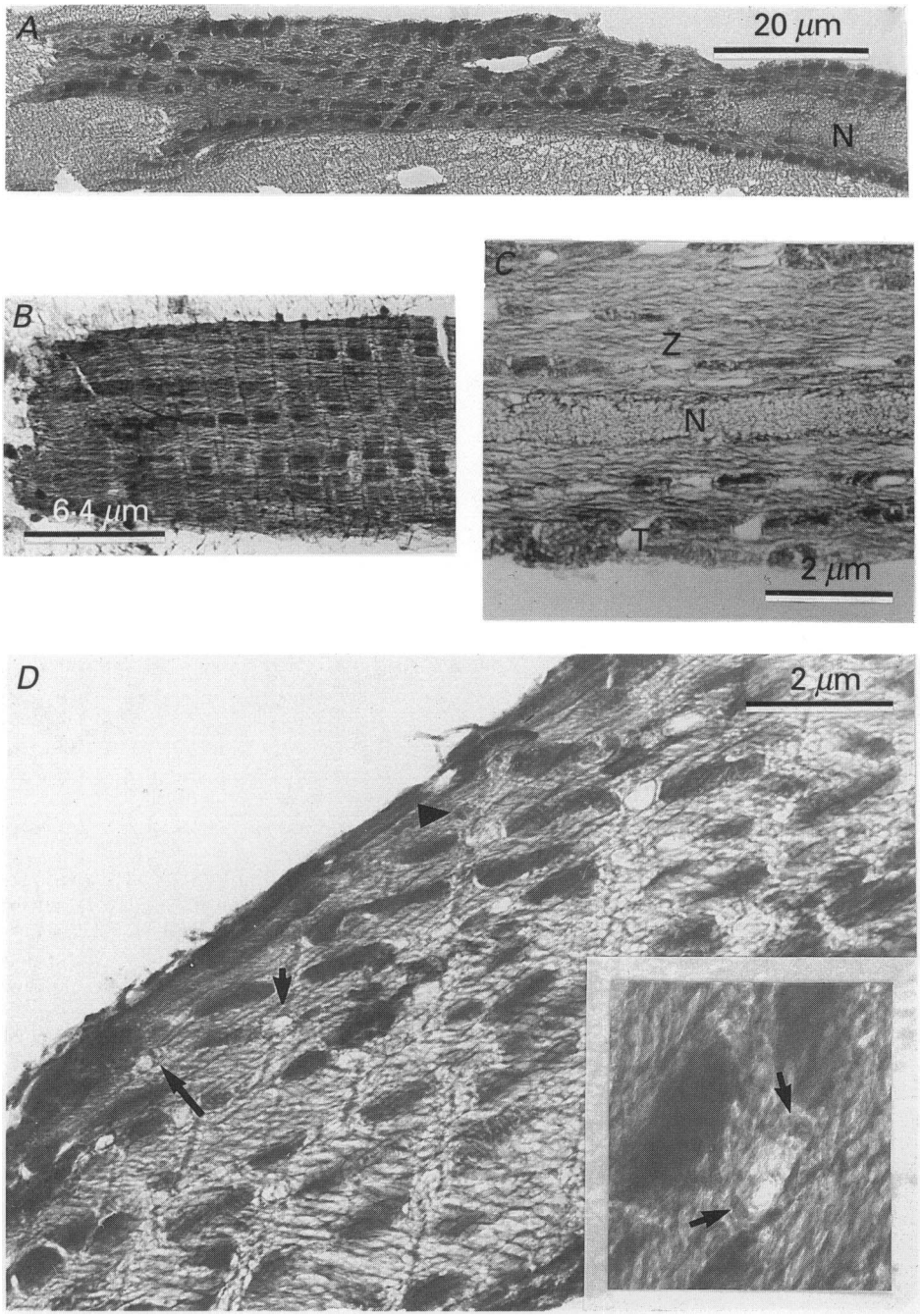

Fig. 3. Cryosections in diastole and systole. *A*, low magnification of part of a longitudinal cryosection obtained from a myocyte frozen during diastole. Nucleus (N), T-tubules (T), sarcomeres, mitochondria, and Z-lines are recognizable. The cell is surrounded by the frozen bath solution. *B*, part of a longitudinal cryosection frozen during systole (sarcomere length 1·65 μm). The section is considered longitudinal since both cell ends

current trace that were used for timing. Service of the magnetic valves induced spiky artifacts in the current trace (paired arrows in Fig. 2). Contact of the cell with the coolant induced a negative spike followed by a large positive current (large arrow in Fig. 2). The position of this artifact in relation to the start of the clamp step to +5 mV allowed us to measure the exact time when shock-freezing occurred.

Cryosectioning. The silver holder containing the cell was stored in frozen solid propane until cryosectioning. The silver holder was mounted under liquid nitrogen in an aluminium holder constructed for the LKB cryoultramicrotome. The specimens were cut at temperatures between −140 and −160 °C into 100–150 nm thin sections. The sections included the myocyte, the surrounding bath solution, and part of the silver holder. The cryosections were picked up dry on copper grids (50 meshes), were freeze-dried under high vacuum overnight, carbon coated, and finally analysed. Representative examples of cryosections of myocytes shock-frozen at diastole and systole are shown in Fig. 3.

Quantitative analysis. The cryosections were mounted in a specimen holder cooled at −100 °C (Gatan Inc., NC, USA). They were analysed in a Philips CM12 STEM electron microscope equipped with a LaB_6 filament, a goniometer stage and a 30 mm^2 Link energy dispersive Si-detector connected to a Link multichannel analyser and a Link 860-500 full quantitative analytical system. The freeze-dried sections were analysed in the STEM-mode with 100 kV acceleration voltage. The analysing beam could be focused to a minimum diameter of 16 nm. For the analysis of the A-band (ΣCa_{myo}), the analysing area was a 1·4 μm long and 0·8 μm wide rectangle so that components of the Z-lines were excluded.

The X-ray spectrum consists of two components: peaks characteristic of the elements present in the analysed microvolume, and a background proportional to the total analysed mass. The ratio between characteristic and continuum counts is linearly related to the concentration (mass fraction) of an element in the analysed volume (Hall, 1979). The 'Quantem' program of the Link analytical system is based on the characteristic continuum theory of Hall (1979), and was used to calculate the concentrations of the elements with atomic number $\geqslant 11$ (Na) in mmol (kg dry weight)$^{-1}$. To obtain the number of counts in a given peak, the program compares a multiple least-squares fit of the filtered spectrum to a library of primary reference files containing pure element spectra. The location of the peak centroid and the resolution of the detector were calibrated by a computer fitting program which determines centroid position and resolution (full weight at half-maximum = FWHM) of two peaks. To avoid errors in the quantitation of elements, the detector gain and the zero line were recalibrated with a centroid position of the peaks within 1 eV each day before the actual analysis.

Peak counts are subject to statistical Poisson error, and the background counts contribute to statistical error in concentration measurements. The 'Quantem' program corrects the background by subtracting the extraneous components due to film, grid, and holder. Furthermore, since the $K_{k\beta}$ peak (potassium X-rays generated from electron orbit $k\beta$) and $Ca_{k\alpha}$ peak (calcium X-rays generated from electron orbit $k\alpha$) partially overlap, and since in the intracellular space potassium concentrations are *ca* 100 times higher than the calcium concentrations, errors in quantitation may become large when processing spectra with high potassium and low calcium concentrations. The partial overlap of the $K_{k\beta}$ peak with the $Ca_{k\alpha}$ adds background of the potassium peak under the calcium peak and may also introduce a systematic error due to inclusion of potassium counts in the calcium peak. The inclusion of the first and second derivative of the potassium peaks in the multiple least-squares reference file (Kitazawa, Shuman & Somlyo, 1983) minimizes errors in quantitation due to partially overlapping peaks, such as $K_{k\beta}$ and $Ca_{k\alpha}$, in case the peak centroid has shifted or the resolution of the detector has decreased during analysis. We have shown (Fig. 4) that in our measurements there is no significant correlation coefficient ($r = 0{\cdot}10$) for the potassium and calcium values. The continuum region selected was 1·36–1·64 keV.

In order to bring the statistical error of the single measurement down to low values (S.D. = ±0·7–0·9 mmol (kg DW)$^{-1}$, even in the case of low concentrations of calcium (when the ratio peak/continuum is close to zero), depending on the thickness of the section, long analysis times are

show the intercalated discs. *C* and *D*, longitudinal crysections of myocytes frozen during diastole. At higher magnifications, junctional SR (arrows) and corbular SR (arrow-head) can be recognized in better-frozen regions of the section. The inset shows a T-tubulus with well-resolved junctional SR (arrows).

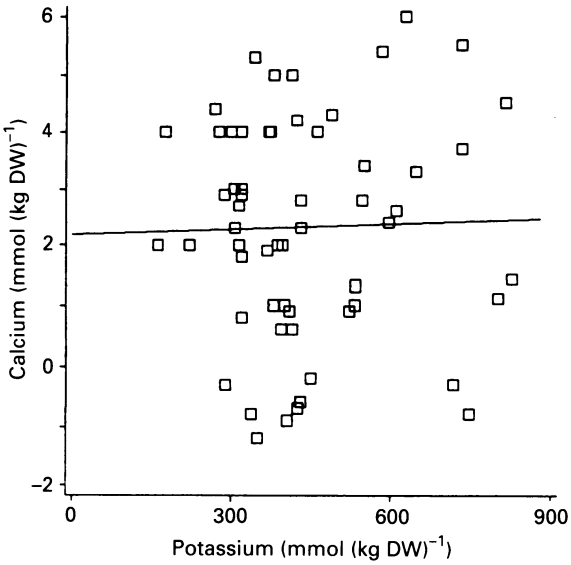

Fig. 4. Scatterogram of calcium and potassium concentrations measured over the myofibrils (A-band). There is no correlation between the potassium and calcium values even though the peaks partially overlap. The correlation coefficient ($r = 0{\cdot}10$) for calcium and potassium values is not significant.

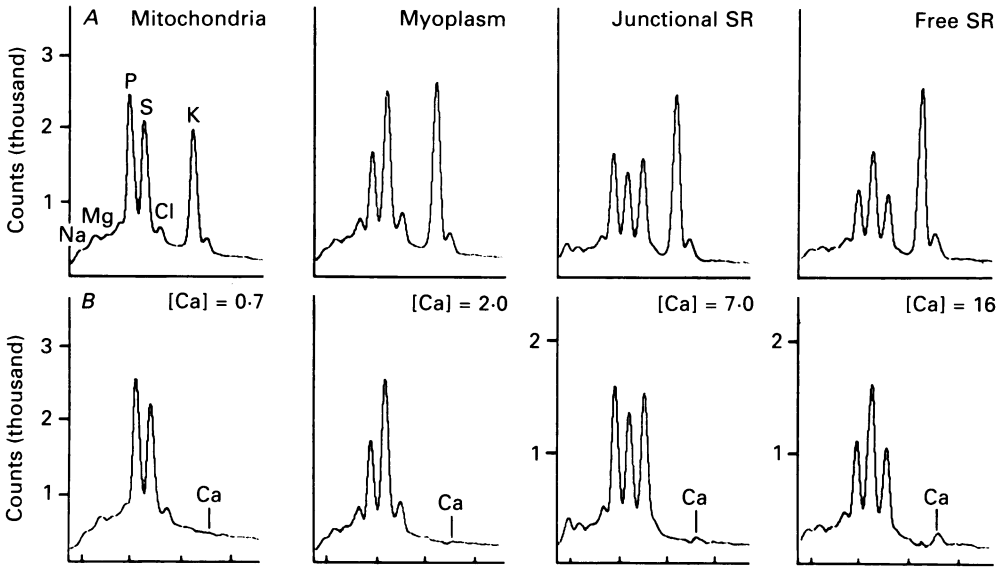

Fig. 5. *A*, spectra collected in mitochondria, myoplasm (myofibrillar region), junctional SR and free SR during 600–1000 s. *B*, after the potassium (K) peaks have been stripped away from the spectrum by the computer, the calcium (Ca) peak becomes clearly visible for concentrations larger than 2 mmol (kg DW)$^{-1}$. Note that the gain for spectra of junctional SR and free SR is higher than for the same spectra in the top row. [Ca] values are in mmol (kg DW)$^{-1}$.

necessary. With analysis times of 600–1000 s, the minimal detectable concentrations of calcium under our conditions are in the range of 0·3–0·5 mmol (kg DW)$^{-1}$. This corresponds to 0·08–0·12 mM-calcium. In the potentiated myocytes, ΣCa of myoplasm, SR, and mitochondria, was in the range of 1·5 mmol (kg DW)$^{-1}$ or more ($\geqslant$ 0·5 mM). Such concentrations are significantly different from zero (95% confidence level) and well above the minimal detectable concentrations. Therefore the accuracy of the ΣCa measurements does not pose serious problems for the present experiments on potentiated myocytes. In Fig 5, examples of spectra are shown before and after the high potassium (K) peaks have been subtracted, in order to make visible the small calcium (Ca) peaks. The corresponding calcium concentrations are indicated.

Quantitative data was transferred from the Link-computer to a PC and statistically evaluated with a SAS statistic package (SAS Inc, NC, USA). To take into account differences in concentrations due to cell-to-cell variance, nested analysis of variance for unbalanced groups was performed. If the overall F test was significant ($P < 0{\cdot}05$), differences between the single groups were then tested by linear comparison (Tukey–Kramer test) and considered significant if $P < 0{\cdot}05$.

Concentration units. EPMA analyses ΣCa per dry weight (mmol (kg DW)$^{-1}$) of the analysed compartment. In order to compare these concentrations with the salt concentration in the patch electrode solution, or with data in the literature, they were transferred into units of molarity (mM) or molality (mmol/kg water) of the analysed compartment. For example, there are good measurements of the water content of mitochondria which is 66% (Werkheiser & Bartley, 1957; Somlyo, Gonzales-Serratos, Shuman, McClennan & Somlyo, 1981). Thus, ΣCa_{mito} of 1 mmol (kg DW)$^{-1}$ can be translated into 0·33 mM (mmol/l mitochondria) or into 0·5 mmol/kg mitochondrial water. For the myofibrillar space (A-band), the water content is less sure; the usual estimates are 75% (Polimeni, 1974). Hence, ΣCa_{myo} of 1 mmol (kg DW)$^{-1}$ corresponds to 0·25 mM or to 0·33 mmol/kg water. The water content in the sarcoplasmic reticulum (SR) has not been published.

Unknown hydration values, as in the SR, can be estimated on the basis of the known mitochondrial water; the X-ray continuum measured in SR, or in the A-band, was compared with the continuum in adjacent mitochondria using the same dose of the electrons (i.e. the same count time and beam intensity). For example, the continuum was 10700 counts in the mitochondria, 9000 in the SR and 8000 in the myofibrillar space. In reference to 66% water in the mitochondrial volume, we estimate for Σ_{myo} a conversion factor of $0{\cdot}24 \pm 0{\cdot}02$ which is nearly identical to the 0·25 given above. For Σ_{SR} the conversion factor was $0{\cdot}28 \pm 0{\cdot}07$; the large S.E.M. is probably due to the fact that the lumen of the SR can be collapsed (high continuum from the lipids) or open (low continuum).

The spatial resolution of subcellular compartments is limited by the diameter of the electron beam obtainable in the microscope and by the thickness of the cryosections. Since in modern microscopes the minimal beam diameter is no longer limiting, it is the 100–150 nm thickness of the cryosections that may preclude analysis of small compartments when the section is thicker than the diameter of the analysed structure (e.g. membrane vesicles, or SR tubules with a narrow lumen). In this paper, we primarily discuss ΣCa_{myo} measured in the A-bands. In this compartment, the spatial resolution of analysis is not limited by the thickness of the section and, generally, the morphology of the A-band is easily recognizable in cryosections. The same is the case for measurements in the mitochondria.

The effective diameter of the analysing beam results in the optimally adjusted microscope from the diameter of the aperture of condensor 2 and from the spot size of the objective lense. In this study, we used a beam with a diameter of 16 nm in the scanning transmission mode (STEM). The size of the area scanned by the beam was chosen depending on the structures to be analysed. If not stated differently, for analysis of the A-band region an area of $1{\cdot}4 \times 0{\cdot}8$ μm was used. For analysis of the region of the Z-lines the area was $0{\cdot}2 \times 0{\cdot}8$ μm. For analysis of SR, the scanning area was reduced to fit if possible inside the SR lumen. For the mitochondria, depending on their size, we used a scanning area in the range of $0{\cdot}5 \times 0{\cdot}5$ μm. During systole, the identification and analysis of subcellular structures became difficult in about 50% of the cryosections, when cell shortening had moved the cell edges away from the Pioloform film on which they were lying during diastole. As a result, those cryosections were no longer longitudinal with the result that the Z-lines were not clearly visible. In the other 50%, however, sufficent morphological resolution was obtained. Figure 3*B* shows a cryosection where, despite sarcomere shortening to 1·66 μm, the cell structures with the Z-bands, M-lines and SR are well resolved.

RESULTS

Potentiation of contraction by paired pulsing

In guinea-pig ventricular myocytes, the amplitude of contraction increases with stimulation frequency. *In vivo*, the heart is beating at a rate of about 3 Hz. Since the computer-controlled experiments are usually done at 1 Hz, contraction was potentiated with a paired-pulse protocol (Fig. 6). In the present study, we analysed only the first contraction during the clamp step to +5 mV.

Paired pulses increased the peak force in a beat-to-beat fashion; potentiation became steady within about five beats (Fig. 6). The potentiated contraction started after a latency of about 15 ms, peaked within about 110 ms and relaxed within 200 ms to 80%. In four myocytes we observed the effect of paired pulsing on unloaded shortening. In the potentiated state, the extent of shortening was 10·3% on average, which corresponds to an average systolic sarcomere length of 1·66 μm. In addition, potentiation slightly reduced the diastolic sarcomere length from 1·85 to 1·82 μm. When paired pulsing was ended, the sarcomere length recovered to the resting 1·85 μm along a half decay time of 1·6 ± 0·4 s.

The $[Ca^{2+}]_i$ transient in the potentiated state

The myoplasmic concentration of free calcium ($[Ca^{2+}]_i$) of unstimulated cells was 95 ± 25 nM on average (mean ± S.E.M. n = 15). During paired pulsing, diastolic $[Ca^{2+}]_i$ increased to 180 ± 41 nM (n = 15, 'diastolic $[Ca^{2+}]_i$ staircase', see Fig. 7; compare Lee & Clusin, 1987). Paired pulsing increased the peak $[Ca^{2+}]_i$ in a beat-to-beat fashion. When potentiation was steady, depolarization to +5 mV induced a rise of $[Ca^{2+}]_i$ that peaked within 25 ± 5 ms to 890 ± 220 nM (see Fig. 9). At on-going depolarization, $[Ca^{2+}]_i$ fell to 50% within about 140 ms. During the second pulse to +50 mV, the decay of $[Ca^{2+}]_i$ became retarded. During the following diastole (600 ms repolarization to −80 mV) $[Ca^{2+}]_i$ fell with enhanced rate. However, the diastole was too short for the return of $[Ca^{2+}]_i$ to the resting value (see above). When pulsing was ended, $[Ca^{2+}]_i$ promptly fell to the resting level with a half-decay time of 1·6 ± 0·2 s.

Elemental distribution in potentiated cells

Using EPMA, we analysed the elements in a population of seventeen cells (seven animals) that were potentiated by at least ten paired voltage clamp pulses. Shock-freezing was timed at the end of the 600 ms long diastole, i.e. 40 ms before a next pulse would have elicited a new systole (see Fig. 2*A*). Table 1 shows the results from 218 spectra. The myofibrillar space was analysed with the electron beam located on the overlapping myofilaments (A-band). The concentrations were measured in mmol (kg DW)$^{-1}$, for comparison with the electrolytes in the patch pipette they were converted into mmol (kg myofibrillar water)$^{-1}$ (factor 0·25, see p. 357). The myoplasmic content of sulphur (S) and phosphorus (P) stems from the proteins. Near the tip of the electrode, the elemental concentrations were very similar to those measured far away at the cell edge. The potassium concentration was 444 mmol (kg DW)$^{-1}$. When converted to 148 mmol (kg myofibrillar water)$^{-1}$, ΣK_{myo} was close to the 145 mM-potassium in the electrode solution. Also, the ΣNa_{myo} of 14 mmol (kg cell water)$^{-1}$ resembled the 10 mM-sodium in the electrode solution. During systole, ΣNa_{myo} was

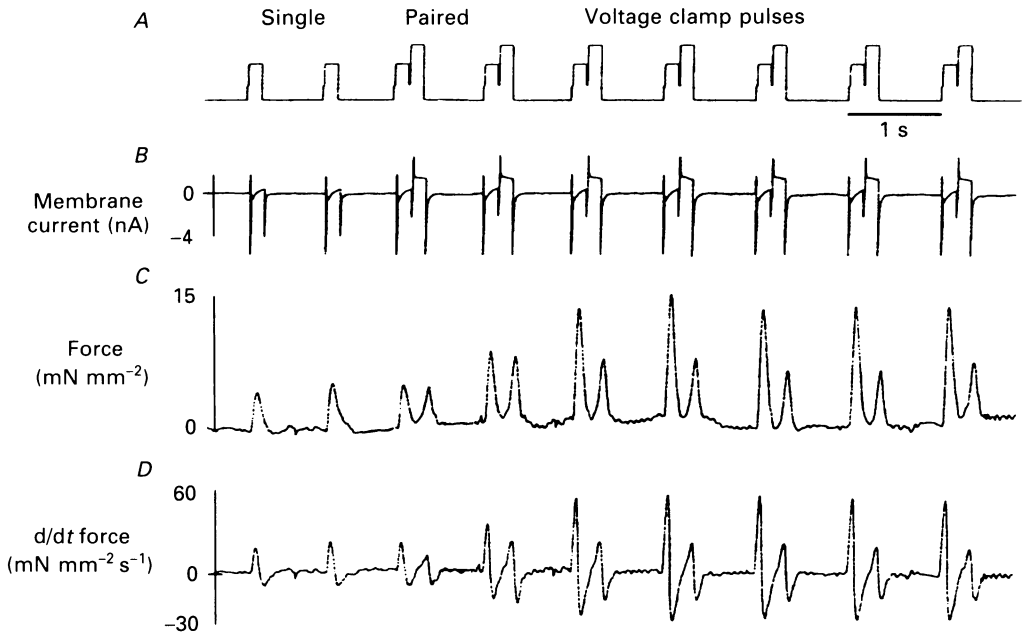

Fig. 6. Paired voltage clamp pulses potentiate contraction. *A*, voltage clamp protocol showing the change from single to paired pulses. (For details of the durations and voltages see Fig. 2.) *B*, membrane current. *C*, isometric force. *D*, derivative of force. Traces are filtered at 30 Hz. Note that the second pulse to +50 mV potentiates the twitch during the depolarization to +5 mV by a factor of 3.

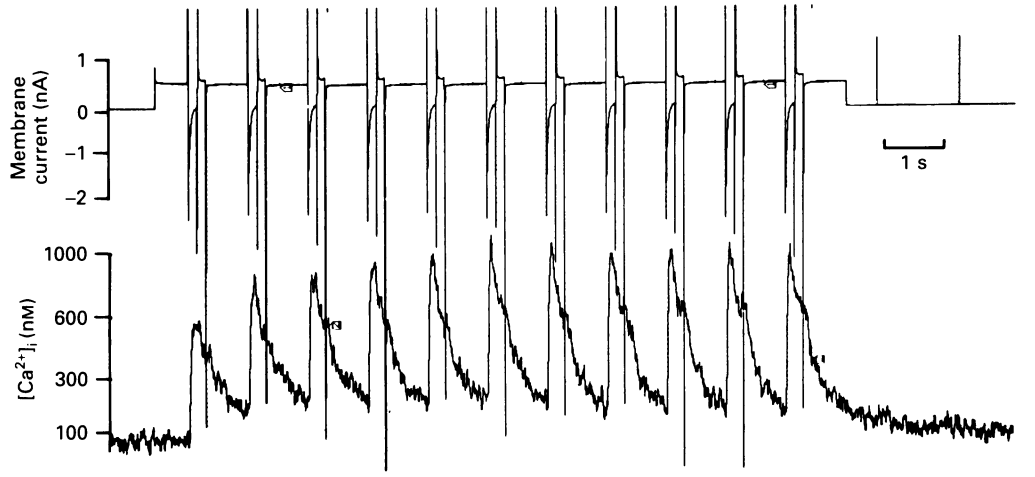

Fig. 7. Membrane currents (top) and changes in $[Ca^{2+}]_i$ (bottom) induced by 1 Hz paired pulsing. $[Ca^{2+}]_i$ of the unstimulated cell (rest period of 4 min) is about 95 nM. Paired pulsing increases diastolic $[Ca^{2+}]_i$ from 95 to 200 nM and the systolic peak of $[Ca^{2+}]_i$ from 600 to 1050 nM. On-line pen recording, $[Ca^{2+}]_i$ filtered at 50 Hz. For $[Ca^{2+}]_i$ measurements cells were loaded with 50 μM-Indo-1 from the pipette. An analogous circuit performed the subtraction of autofluorescence and fluorescence ratio (490 nm/410 nm) on-line.

19 mmol (kg water)$^{-1}$ which is not significantly different to diastolic ΣNa_{myo}. Close to the surface sarcolemma, ΣNa_{myo} could be significantly higher than in the middle of the cell (up to 75 mmol (kg water)$^{-1}$, Isenberg & Wendt-Gallitelli, 1990). Peculiarities of those intracellular sodium gradients will be considered in a forthcoming paper. ΣMg_{myo} was 12 mmol (kg myofibrillar water)$^{-1}$ during diastole and 14 mmol (kg

TABLE 1. Elemental concentration obtained by EPMA end-diastolic after paired pulsing

	n	Na	Mg	P	S	Cl	K	Ca
A		Concentrations in millimoles per kilogram dry weight (mmol (kg DW)$^{-1}$) (±S.E.M.)						
Myoplasm	62	43±5	36±2	339±14	352±18	152±19	444±22	2·6±0·4
SR	93	73±8	35±2	388±13	284±15	203±14	428±21	8·6±1·3
Mitochondria	50	25±5	21±1	426±15	246±15	103±12	278±16	1·3±0·2
B		Concentrations converted to millimoles per kilogram water in the compartment						
Myoplasm		14	12	113	117	51	148	0·9
SR		27	13	144	100	75	158	3·2
Mitochondria		12	10	213	123	51	139	0·65
C		Concentrations converted to millimolar (mM) or mmoles per litre compartment						
Myoplasm		11	9	85	88	38	111	0·65
SR		20	10	108	80	57	120	2·4
Mitochondria		8	7	142	82	34	93	0·4

A, elemental concentrations in sarcoplasmic reticulum (SR), mitochondria and myoplasm as given by the Quantem program of the analytical system, which calculates concentrations as mass fractions (of the continuum). B the concentrations in myoplasm, SR and mitochondria have been transformed into millimoles per kilogram cell water. C, the concentrations have been transformed into millimoles per litre analysed compartment. A water content of 66% was assumed in the mitochondria and 75% in the myoplasm. Data stem from seventeen guinea-pig ventricular myocytes. During the experiment, the cells were continuously superfused with a 36 °C warm salt solution composed of 150 mM-NaCl, 5·4 mM-KCl, 2 mM-$CaCl_2$, 1·2 mM-$MgCl_2$, 5 mM-glucose, 5 mM-HEPES/NaOH (pH 7·4).

water)$^{-1}$ during systole. ΣMg_{myo} of 12 mmol (kg water)$^{-1}$ was compared with 0·5 mM free $[Mg^{2+}]_i$ (ion-sensitive electrodes; Blatter & McGuigan, 1986), 95% of the total ΣMg_{myo} seemed to be bound. The ΣCl_{myo} of 49 mmol (kg myofibrillar water)$^{-1}$ was only 30% of the 162 mM-chloride in the electrode solution, the difference could suggest that negative charges of intracellular proteins modify the distribution of Cl^- ions (Donnan effect). During systole, ΣCl_{myo} increased significantly ($P < 0·01$) to 109±21 mmol (kg water)$^{-1}$. These changes in ΣCl are outside the scope of this paper.

The mitochondria were easy to recognize and to analyse. In reference to dry weight, mitochondrial concentrations were lower than their counterparts in the myofibrillar space. However, the water content is lower in mitochondria than in the myoplasm, and transformation of the concentration to mmoles per kilogram mitochondrial water brought the elemental concentrations in mitochondria and myoplasm to nearly identical values (see Table 1). Only the phosphorus (P) concentration was higher in the mitochondria than in the myofibrillar space, as can be expected.

The sarcoplasmic reticulum (SR) was analysed in the region of the Z-lines. Since some SR structures had dimensions smaller than the 100–150 nm thickness of the cryosection, the analysis comprised not only elements stored in the lumen of the SR and bound to the SR membrane, but also, possibly, elements in a fringe of myoplasm

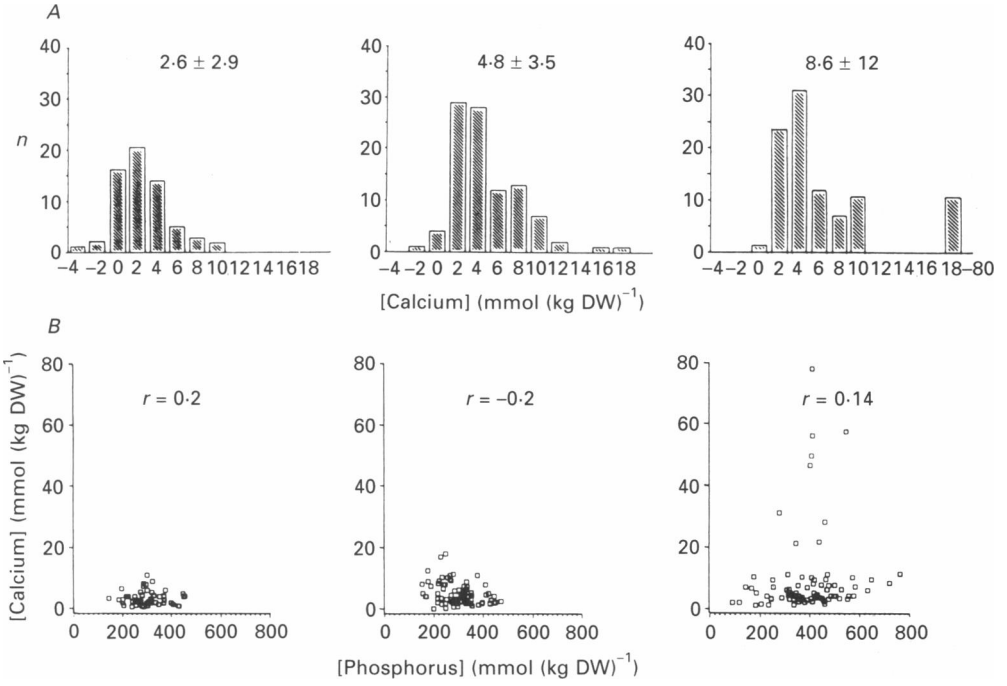

Fig. 8. Frequency distribution of calcium concentrations. *A*, diastolic ΣCa_{myo} (left panel) and systolic ΣCa_{myo} (15–25 and 30–45 ms, middle panel), as well as diastolic ΣCa_{SR} (right panel); mean ± S.D. shown in each panel. *B*, correlation between calcium and phosphorus concentrations. Diastolic ΣCa_{myo} (left panel), systolic ΣCa_{myo} (15–25 and 30–45 ms, middle panel) as well as diastolic ΣCa_{SR} (right panel). Note there is no correlation between the high ΣCa_{myo} and ΣP_{myo} during systole. Therefore the possibility can be excluded that the high ΣCa_{myo} stems from measurements including the SR membranes with high phosphorus.

adjacent to these organelles (see Discussion). Typically, the junctional SR had concentration of phosphorus higher than the myoplasm, probably due to the contribution of phospholipids (compare Joergensen, Broderick, Somlyo & Somlyo, 1988). Table 1 shows that ΣK_{SR} and ΣMg_{SR} were similar to that of the surrounding myoplasm, whereas ΣNa_{SR} and ΣCl_{SR} were significantly higher. The calcium concentration will be evaluated below.

Distribution of ΣCa during diastole

At the end of diastole, the myofibrillar space contained a ΣCa_{myo} of 2·6 ± 0·4 mmol (kg DW)$^{-1}$ ($n = 62$, see the frequency distribution of Fig. 8). Since ΣCa_{myo} of unstimulated myocytes was not different from zero (Wendt-Gallitelli &

Isenberg, 1989), we interpret that ΣCa_{myo} increased during the potentiation of contraction. Most of ΣCa_{myo} is thought to be bound to proteins, and therefore the concentration per kilogram dry weight was converted to mM (mmoles per litre myofibrillar space). In terms of molarity, diastolic ΣCa_{myo} was 0·65 mM, a value 3611 times higher than the 0·18 μM free $[Ca^{2+}]_i$ measured by Indo-1 technique. That is, only 0·03 % of ΣCa_{myo} was ionized and 99·97 % was bound.

TABLE 2. Time course of ΣCa measured by EPMA in myoplasm, SR and mitochondria. The concentrations were measured in millimoles per kilogram dry weight and converted into millimoles per litre of analysed compartment (mM). *n* gives the number of spectra, of cells, and of animals. Significant differences in ΣCa are marked by < > for $P < 0.05$ and by ≪ ≫ for $P < 0.01$. The letters A, B and C indicate the compartments and the numbers 1, 2, 3 and 4 the functional states to which the difference is significant

	Diastole (1)	Early systole (15–25 ms) (2)	Middle systole (30–45 ms) (3)	Late systole (60–120 ms) (4)
Myoplasm (A)	(A, 1)	(A, 2)	(A, 3)	(A, 4)
Significance *versus*		≪ A, 1 ≫	≪ A, 1 ≫	
		≪ A, 4 ≫	≪ A, 4 ≫	
n	(62, 17, 7)	(35, 4, 4)	(58, 6, 5)	(33, 3, 2)
mmol (kg DW)$^{-1}$ ± S.E.M.	2·6 ± 0·4	5·5 ± 0·3	4·6 ± 0·5	3·1 ± 0·5
Converted to mM	0·65	1·4	1·15	0·8
SR (B)	(B, 1)	(B, 2)	(B, 3)	(B, 4)
Significance *versus*	≪ B, 2 ≫			
	≪ A, 1 ≫		≪ A, 3 ≫	
	< C, 1 >		≪ C, 3 ≫	< C, 4 >
n	(93, 17, 7)	(13, 4, 3)	(24, 6, 5)	(13, 3, 2)
mmol (kg DW)$^{-1}$ ± S.E.M.	8·6 ± 1·3	4·1 ± 0·4	7·2 ± 0·9	5·4 ± 0·6
Converted to mM	2·4	1·1	2·0	1·5
Mitochondria (C)	(C, 1)	(C, 2)	(C, 3)	(C, 4)
Significance *versus*		≪ A, 2 ≫	≪ C, 1 ≫	
n	(50, 17, 7)	(8, 4, 2)	(26, 6, 5)	(11, 3, 2)
mmol (kg DW)$^{-1}$ ± S.E.M.	1·3 ± 0·2	1·7 ± 0·4	3·7 ± 0·5	1·7 ± 0·8
Converted to mM	0·4	0·5	1·2	0·5

During diastole of potentiated myocytes, mitochondrial ΣCa_{mito} was 1·3 mmol (kg DW)$^{-1}$ or 0·4 mM. Although this value is lower than ΣCa_{myo}, the difference between ΣCa_{myo} and ΣCa_{mito} is not significant. However, diastolic ΣCa_{mito} was significantly larger than zero ($P < 0.05$). In the sarcoplasmic reticulum, ΣCa_{SR} was 8·6 ± 1·3 mmol (kg DW)$^{-1}$ or 2·4 mM ($n = 93$) which is significantly higher than diastolic ΣCa_{myo}. Most probably, this difference is an underestimate (see p. 369).

ΣCa_{myo} *during systole*

We analysed cells frozen 15, 20, 25, 30, 40, 45, 60, 90 and 120 ms after the start of depolarization. For statistical analysis, data were packed into groups of 15–25 ms (early systole, 56 spectra), 30–45 ms (middle systole, 113 spectra) and 60–120 ms (late systole, 60 spectra). Since we were mostly interested in the early moment of systole where the rapid changes in $[Ca^{2+}]_i$ occur, most cells ($n = 10$) were shock-

frozen at early and middle systole. In about 50% of the cryosections, the sarcomeres were clearly visible and ΣCa_{myo} was analysed in the A-band (Fig. 9). In the other 50% ΣCa_{myo} was considered to be 'myoplasmic' if the ΣP_{myo} was lower than 400 mmol (kg DW)$^{-1}$ (compare Joergenson *et al.* 1988). In Fig. 8 it is shown that

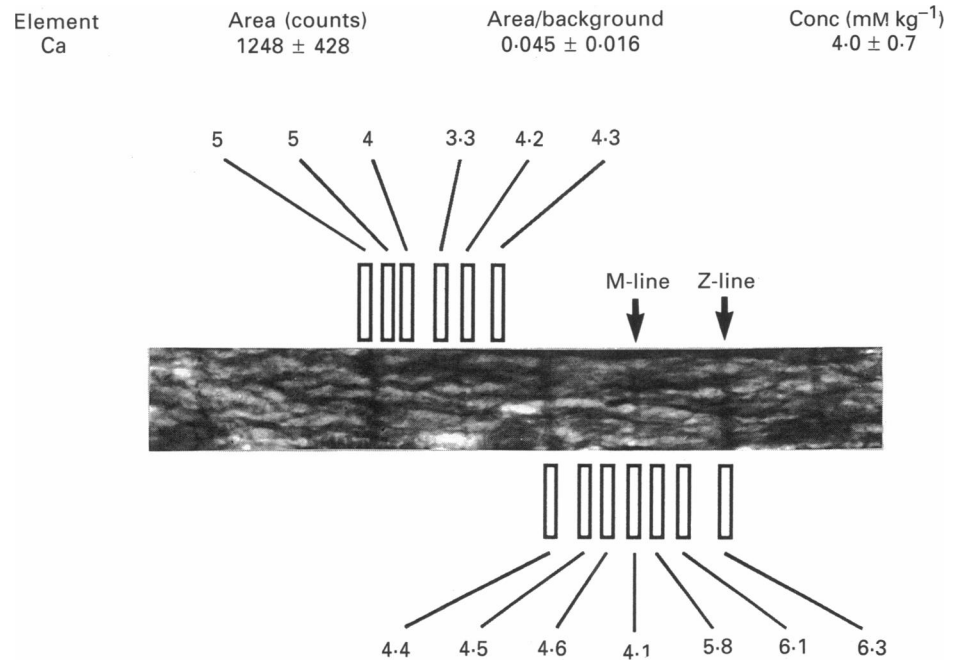

Fig. 9. Representative part of a cryosection from a strongly contracted myocyte (middle systole, part of the cryosection shown in Fig. 3*B*). The Z-lines and the M-line are well recognizable. The analysing scanning area of 0·2 × 0·7 μm (labelled) was placed to different locations of the sarcomere, measured ΣCa_{myo} are indicated in mmol (kg DW)$^{-1}$. Analysis was performed until the error (S.D.) of the single calcium measurement was as low as 0·7 mmol (kg DW)$^{-1}$. One original computer print-out for the calcium is indicated. Area = peak counts.

there is no correlation between the myofibrillar calcium and phosphorus concentrations in the early and middle systole. In particular, the highest ΣCa_{myo} measured during systole showed low phosphorous (*ca* 200 mmol (kg DW)$^{-1}$).

Table 2 shows the values of ΣCa_{myo} measured in the myofibrillar space. During early systole (15–25 ms), ΣCa_{myo} increased to 5·5 mmol (kg DW)$^{-1}$, a value significantly higher than diastolic ΣCa_{myo}. At middle systole (30–45 ms), ΣCa_{myo} was 4·6 mmol (kg DW)$^{-1}$ which is still significantly different from the diastolic ΣCa_{myo}. The late systole includes data measured between 60 and 120 ms. At this time, ΣCa_{myo} was 3·1 mmol (kg DW)$^{-1}$ which is significantly lower than ΣCa_{myo} during early and middle systole, and ΣCa_{myo} was no longer significantly different from the diastolic concentrations. That is, at a time when mechanical systole (shortening) was still continuing, the systolic increase in ΣCa_{myo} had nearly disappeared.

ΣCa_{myo} was converted from mmoles per kilogram dry weight into mmoles per litre myofibrillar space. In these terms ΣCa_{myo} peaked from diastolic 0·65 mM to 1·4 mM (15–25 ms) and fell to 1·15 mM (30–45 ms) and 0·8 mM (60–120 ms), respectively. The increment from diastolic to peak ΣCa_{myo} is 750 μM. To calculate the Ca^{2+}-buffering

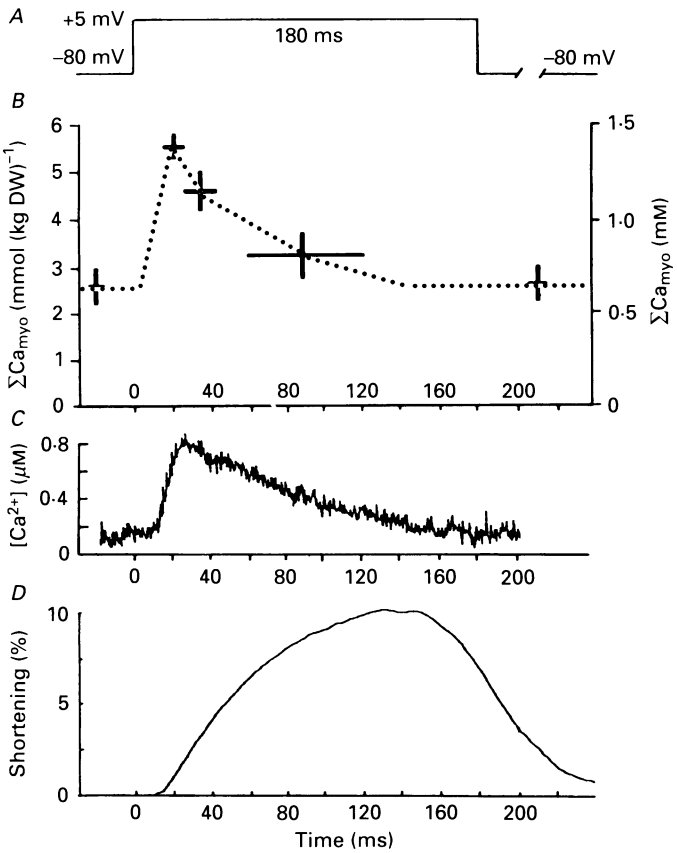

Fig. 10. Time course of ΣCa_{myo} (*B*) in comparison with $[Ca^{2+}]_i$ (*C*) and isotonic shortening (*D*). *A* shows the voltage clamp protocol (pre-pulse to −45 mV not shown for clarity). In *B*, vertical bars indicate S.E.M. of the mean, horizontal bars the period of time where measurements were grouped together. *C* and *D* are averages from ten sweeps. For $[Ca^{2+}]_i$, data are transformed into a linear scale by computer.

capacity of the myofibrillar space, the increment in ΣCa_{myo} is divided by the correspondent increment in $[Ca^{2+}]_i$ (0·71 μM). This ratio is divided by the 0·69 pCa units by which free $[Ca^{2+}]_i$ had changed (from 180 nM or pCa 6·74 to 890 nM or pCa 6·05). The result is a Ca^{2+}-buffering capacity of 1·5 mmol ΣCa_{myo} per pCa unit for $[Ca^{2+}]_i$ between 0·2 and 0·9 μM. Similar millimolar values for the Ca^{2+}-buffering capacity have been reported by Becker, Walsh, Singer & Fay (1988).

Regarding the time course, both ΣCa_{myo} and $[Ca^{2+}]_i$ peaked between 15 and 25 ms. At late systole, the increment in ΣCa_{myo} had fallen to 20% of the peak whereas the increment in $[Ca^{2+}]_i$ was about 60% of the peak. Thus, the decay of $[Ca^{2+}]_i$ seems to

be slower than the decay of ΣCa_{myo}. In part, this could be due to a slow unbinding of Ca^{2+} from Indo-1 (Bayler & Hollingworth, 1988). However, for a detailed comparison of ΣCa_{myo} and $[Ca^{2+}]_i$ during late systole, the number of EPMA time points are not yet sufficient.

The present study also offers a comparison of ΣCa_{myo} and $[Ca^{2+}]_i$ with the time course of cell shortening. Figure 10 shows that both ΣCa_{myo} and $[Ca^{2+}]_i$ peaked at a time when shortening just started. Shortening occurred at maximal rate at 42 ± 15 ms, which is later than the time to peak of ΣCa_{myo} and $[Ca^{2+}]_i$. Contraction peaked at 128 ± 25 ms, a time where ΣCa_{myo} and $[Ca^{2+}]_i$ had largely returned towards the diastolic values. Thus, the time course of contraction does not follow the time course of total or free calcium.

Systolic ΣCa in SR

At early systole (15–25 ms) ΣCa_{SR} was 4·1 mmol (kg DW)$^{-1}$ or 1·15 mM. This concentration did not significantly differ ($P \geqslant 0{\cdot}05$) from ΣCa_{myo}. That is, the concentration difference between ΣCa_{SR} and ΣCa_{myo}, shown for diastole, had disappeared 15–25 ms after start of depolarization. This property is expected from a release compartment. During middle systole (30–45 ms) ΣCa_{SR} increased to 7·2 mmol (kg DW)$^{-1}$ (2 mM), i.e. the difference between ΣCa_{SR} and ΣCa_{myo} became significant again ($P < 0{\cdot}01$). Such a property would be expected if calcium is taken up by the SR. During late systole (60–120 ms), the difference between ΣCa_{SR} and ΣCa_{myo} was without significance, most probably the number of measurements was too small. We will address the question about calcium release from and calcium reuptake into the SR in a forthcoming paper.

Systolic ΣCa in mitochondria

During early systole, ΣCa_{mito} changed from diastolic 0·4 mM to 0·5 mM, this increase was not significant. However, during early systole ΣCa_{mito} was significantly lower than ΣCa_{myo}. During middle systole, this difference disappeared due to an increase of ΣCa_{mito} to 1·2 mM, close to ΣCa_{myo} (1·15 mM). During middle systole, ΣCa_{mito} was significantly higher than during diastole. During the late systole (60–120 ms) ΣCa_{mito} fell to 0·5 mM which is not significantly different from diastole. Our data show that mitochondrial ΣCa can participate in the changes of intracellular calcium during the cardiac cycle, at least under the present experimental conditions. The increase in mitochondrial ΣCa follows the increase in myoplasmic ΣCa with some delay suggesting that ΣCa_{mito} does not cause the increase in ΣCa_{myo} but rather is the consequence of the increase.

DISCUSSION

Our data show that, for a relaxed cell, the concentration of total calcium in the myofibrillar space ΣCa_{myo} is of the order of $2{\cdot}6 \pm 0{\cdot}4$ mmol (kg DW)$^{-1}$, or 0·65 mM. This high ΣCa_{myo} reflects the potentiated state of the myocytes; it was not measured when cardiac ventricular preparations were at rest (Wendt-Gallitelli, 1986; Wendt-Gallitelli & Isenberg, 1989) or stimulated at low frequency ($0{\cdot}6 \pm 0{\cdot}1$ mmol (kg DW)$^{-1}$, Wendt-Gallitelli, 1985; $0{\cdot}5 \pm 0{\cdot}3$ mmol (kg DW)$^{-1}$, Joergenson *et al.* 1988). We think that the potentiated state compares with the *in vivo* situation where

the heart beats at a frequency of 3 Hz or more. In whole hamster hearts beating spontaneously at 4–5 Hz, a diastolic ΣCa_{myo} of $2{\cdot}6 \pm 0{\cdot}4$ mmol (kg DW)$^{-1}$ has been measured (Bond, Jaraki, Disch & Healey, 1989). Without a significant elevation of resting tension, diastolic ΣCa_{myo} was as high as 6 ± 2 mmol (kg DW)$^{-1}$ after the trabeculae had been potentiated by either 0·2 μM-ouabain or 0·1 μM-noradrenaline (1 Hz stimulation, Wendt-Gallitelli, 1986). Thus, the increase of ΣCa_{myo} to more than 2 mmol (kg DW)$^{-1}$ (more than 600 μM) is not a peculiarity of the single-cell preparation or of the potentiation by paired voltage clamp pulses; rather it seems to be a phenomenon generally connected to positive inotropy.

In the present study on isolated ventricular myocytes, potentiation went together with a sarcomere length 2% shorter and a free $[Ca^{2+}]_i$ twofold higher than their counterparts at rest. At the end of paired pulsing, both sarcomere length and $[Ca^{2+}]_i$ promptly relaxed to the resting values with a half-time of about 1·6 s, indicating that the cells were not unspecifically damaged. The results suggest that, during the 600 ms diastole, the redistribution of Ca^{2+} did not reach the rested state values. We interpret these changes as a physiological phenomenon which is causally related to frequency-dependent potentiation ('diastolic staircase', see Lee & Clusin, 1987).

The potentiated state is not the state of 'calcium overload'. The two situations can be distinguished as follows. In the potentiated state, the myocytes contracted and relaxed in the same regular pattern as previously described (Shepherd, Vornanen & Isenberg, 1990). Also, the $[Ca^{2+}]_i$ transients were comparable to those reported in the literature (guinea-pig ventricular myocytes at 22 °C; e.g. Beuckelmann & Wier, 1988). When the myocytes were calcium overloaded (in about 10% of the myocytes, not used for EPMA), calcium overload was indicated by after-contractions and transient inward currents. In calcium-overloaded cells, $[Ca^{2+}]_i$ transiently fell below the 180 nM of the potentiated cells (compare Allen, Eisner, Pirolo & Smith, 1985). Since this 'underswing' was absent during potentiation, we interpret the results to mean that potentiation and calcium overload are different phenomena.

Our results have indicated that 99·97% of total ΣCa_{myo} is bound. Hence, one would like to know the ligand(s). In the literature, calmodulin, troponin C and myosin have been described for the myofibrillar space (e.g. Fabiato, 1983). Significant Ca^{2+} binding to the Ca^{2+}, Mg^{2+} sites of myosin can be excluded: these sites are occupied by magnesium since $[Mg^{2+}]_i$ is 4 orders of magnitude higher than $[Ca^{2+}]_i$ whereas the affinities for Ca^{2+} and Mg^{2+} differ only by a factor of 100. According to the published affinities and rate constants (Robertson, Johnson & Potter, 1981), the Ca^{2+}, Mg^{2+} sites of troponin C would have properties suitable to account for the potentiation-induced increase in diastolic ΣCa_{myo} and $[Ca^{2+}]_i$. The concentration of troponin C, however, is too low. In cardiac homogenates, troponin C has a concentration of 28 μmol (kg tissue wet weight)$^{-1}$ (Solaro, Wise, Shiner & Briggs, 1974). With the assumption of 768 g water (kg tissue wet weight)$^{-1}$, and 25% of total water being extracellular (Polimeni, 1974), one estimates 49 μM-troponin C in the intracellular space. Since troponin C is restricted to the myofibrillar compartment (57% of total cell volume; Page, 1978), the concentration of troponin C is probably 86 μmol (l myofibrillar space)$^{-1}$. Another estimate comes from morphology and X-ray structure analysis (Huxley & Faruqi, 1983). The concentration of troponin C is thought to equal the concentration of myosin heads. Myosin molecules have an

average axial distance of 40 nm, and they have six heads within a periodicity of forty-two. From these numbers one estimates 142 μM-myosin heads per litre myofibrillar space. Since each troponin C has two Ca^{2+}, Mg^{2+} sites, the total number of calcium-binding sites is somewhere between 160 and 280 μM whereas 650 μM-ΣCa_{myo} were measured. Hence we postulate the myofibrillar space to contain, in addition to the Ca^{2+}, Mg^{2+} sites of troponin C, about 600 μM-Ca^{2+}-binding sites. These sites should have on- and off-rates for Ca^{2+} binding similar to those of the Ca^{2+}, Mg^{2+} sites of troponin C. With those additional ligands we can adequately model the potentiation-mediated increase in $[Ca^{2+}]_i$ and ΣCa_{myo} and its decay upon rest. The model predicts for the diastole of potentiated cells that 28% of the calcium-specific sites on troponin C were occupied by calcium, which could account for the observed modest reduction of averaged sarcomere length.

The systolic increment of ΣCa_{myo}

When contraction was potentiated, ΣCa_{myo} peaked within 25 ms to 1·4 mM. The high ΣCa_{myo} raises the question about a possible contamination of ΣCa_{myo} by ΣCa_{SR} in those cryosections where the morphological resolution of the sarcomeres and the SR was not ideal. Contamination of ΣCa_{myo} by ΣCa_{SR} can be excluded in view of the following arguments. The ΣCa_{myo} evaluated from sections with a well-resolved ultrastructure (example of Fig. 9) fell into the same group as the one given in Table 2. Also, any membrane-bearing compartment would have distorted the texture of the myofilaments seen in the cryosections. Finally, ΣCa_{myo} did not correlate with ΣP_{myo} (Fig. 8) indicating that the high ΣCa_{myo} has not been measured in structures with high phosphorus such as SR membranes with their high content of phospholipids.

The systolic peak ΣCa_{myo} of 5·5 mmol (kg DW)$^{-1}$ (1·4 mM) is not unusually high. For example 8 mmol (kg DW)$^{-1}$ was measured in the I-band of tetanized frog skeletal muscles (Somlyo *et al.* 1981). Free $[Ca^{2+}]_i$ peaked during systole to approximately 0·9 μM, which is similar to the values in the literature (e.g. Beuckelmann & Wier, 1988). The ratio between 1·4 mM ΣCa_{myo} and 0·9 μM free $[Ca^{2+}]_i$ is > 1000, or more than 10 times higher than calculated on the basis of known Ca^{2+} ligands. Hence we have to search for ligands that can bind and unbind the systolic increment of 750 μM-ΣCa_{myo} during a time scale of 20 ms. Regarding the rate constants, the calcium-specific site of troponin C would be adequate, provided the published numbers (Solaro *et al.* 1974) could be increased by a factor of 3 to account for the different temperature (36 ° *versus* 22 °C). However, the calcium-specific site of troponin C can bind 100 μM at the best (20% of this is already occupied during diastole, see above). Thus, we postulate that at least 2000 μM additional 'fast' calcium buffer is present in the myofibrillar space. Biochemical data, however, do not suggest what molecule could bear these sites.

The time course of myoplasmic $[Ca^{2+}]_i$ has been measured by aequorin luminescence (e.g. Allen & Kurihara, 1980; Blinks & Endoh, 1986) or microfluospectroscopy (Beuckelmann & Wier, 1988; see also Fig. 10). From such measurements, $[Ca^{2+}]_i$ was shown to peak 20–40 ms after the start of depolarization, and then to decay while the contraction continued to increase. As with the present Indo-1 measurements, those $[Ca^{2+}]_i$ signals were averaged from the whole cell and

they did not provide direct information on how much Ca^{2+} was bound to troponin C. By combining EPMA of ΣCa_{myo} with Indo-1 measurements of free $[Ca^{2+}]_i$, we have shown that the $[Ca^{2+}]_i$ signal does not decay because Ca^{2+} shifts from the indicator to troponin C ('upstream'; see Blinks & Endoh, 1986). In contrast, $[Ca^{2+}]_i$ decays because it is sequestered into the SR ('down-stream'; see Allen & Kurihara, 1980). That is, ΣCa over the overlapping filaments was significantly reduced as early as 60–120 ms after the start of depolarization (Table 2). Thus, Ca^{2+} binds to these structures only during a short period. Most importantly, myoplasmic total calcium falls rapidly before contraction has reached its peak. Provided that ΣCa_{myo} reflects calcium bound to the calcium-specific site of troponin C, the lifetime of this activation complex is shorter than the time required for the contraction to peak. The rapid time course of $[Ca^{2+}]_i$ and ΣCa_{myo} indicates that is not the lifetime of the calcium–troponin C complex, but the turnover rate of the cross-bridges that limits the timecourse of contraction.

Mitochondria

In the present experiments with potentiated myocytes, diastolic ΣCa_{mito} was significantly larger than zero (1·3 mmol (kg DW)$^{-1}$ or 0·4 mM). Since unstimulated cells did not contain significant ΣCa_{mito} (Wendt-Gallitelli & Isenberg, 1989), we interpret that diastolic ΣCa_{mito} increased as a consequence of the long-lasting increase in ΣCa_{myo}, induced by potentiation. However, in multicellular ventricular preparations, elevated diastolic ΣCa_{mito} has not been reported up to now. Not only unpotentiated ventricular trabeculae have a ΣCa_{mito} below the detection limit (Wendt-Gallitelli, 1986; Joergensen *et al.* 1988). In guinea-pig ventricular trabeculae potentiated with paired pulses (Wendt-Gallitelli, 1986) or in hamster hearts beating at 4 Hz (Bond *et al.* 1989), ΣCa_{mito} was not significantly different from zero. On the other hand, significant mitochondrial calcium-uptake load during potentiation was measured in guinea-pig papillary muscles using ^{45}Ca (Lewartowski & Pytkowski, 1987).

During systole ΣCa_{mito} followed ΣCa_{myo} with a 40 ms time lag. The systolic increase in ΣCa_{mito} was a short-lasting phenomenon which would not have been recorded when the preparations were shock-frozen at the peak of contraction (Table 2), and EPMA of ΣCa_{myo} timed at 30–45 ms after start of excitation has not been reported up to now. However, significant uptake and egress of mitochondrial calcium during the cardiac cycle has been calculated by extrapolation of measurements of calcium shifts in suspensions of isolated ventricular myocytes (Fry, Powell, Twist & Ward, 1984; Fry, Harding & Miller, 1989). One is tempted to speculate that the transient changes of ΣCa_{mito} are involved in the calcium regulation of mitochondrial enzymes during the contraction cycle (Krause *et al.* 1987; McCormack, Halestrap & Denton, 1990). To find out whether the present mitochondrial Ca^{2+} movements are compatible with data on Ca^{2+} influx and efflux measured in isolated mitochondria, we translated the changes in ΣCa_{mito} into a rate of mitochondrial Ca^{2+} influx. With 70% protein per dry mass (Somlyo, Bond & Somlyo, 1985), we obtained a rate of 4·3 μmol min^{-1} (mg protein)$^{-1}$ for 36 °C which is compatible with maximal rates of 1·7 μmol min^{-1} (mg protein)$^{-1}$ measured in isolated cardiac mitochondria at 22 °C (McMilin-Wood, Wolkowicz, Chu, Tate, Goldstone & Entman, 1980). It has been argued that the Ca^{2+} affinity of the uniporter is too low for significant Ca^{2+} accumulation of submicromolar

$[Ca^{2+}]_i$. However, due to the 2 mM-spermine in cardiac cells (Persson & Rosengren, 1983) the K_m could be 200 μM or lower (Nicchitta & Williamson, 1984). Thus, data about Ca^{2+} influx in isolated mitochondria seem to be compatible with the present measurements. For the egress of mitochondrial Ca^{2+}, however, our data suggest a rate of 400 nmol min^{-1} (mg protein)$^{-1}$, whereas in isolated mitochondria rates of about 20 nmol min^{-1} (mg protein)$^{-1}$ have been reported (22 °C; Crompton, Moser, Lüdi & Carafoli, 1978). One could speculate that the large and rapid egress of ΣCa_{mito} observed here in the whole cell is due to stimulation by some unknown cytosolic 'factor' (like spermine) which is lost during the isolation of mitochondria. On the other hand, one could argue that the present rapid mitochondrial calcium shifts were measured in isolated dialysed myocytes, representing a peculiar experimental condition which cannot be extrapolated. Thus, the question whether the significant mitochondrial calcium shifts are of physiological importance *in vivo*, remains to be clarified in the future.

Calcium in the sarcoplasmic reticulum

The 750 μM systolic increment in ΣCa_{myo} requires a source that can provide large amounts of calcium at a high rate. Influx of extracellular calcium has been estimated from the time integral of calcium channel current I_{Ca}. Up to the moment of 'early systole', I_{Ca} increments ΣCa_{myo} by about 50 μM (Isenberg, 1982; Wendt-Gallitelli & Isenberg, 1989) which is too low by one order of magnitude. Since Ca^{2+} influx was too low, the increment in ΣCa_{myo} was assumed to stem from an intracellular Ca^{2+} store (see, Fabiato, 1983; Callewaert, Cleeman & Morad, 1988).

One would like to identify the 'functional Ca^{2+} store' with a morphological structure such as the SR. Using EPMA, ΣCa_{SR} can be shown to have the properties expected from the functional Ca^{2+} store (Wendt-Gallitelli, Jacob & Wolburg 1982; Wendt-Gallitelli, 1985, 1986; Wheeler-Clark & Tormey, 1987; Joergensen *et al.* 1988; Bond *et al.* 1989). During diastole, ΣCa_{SR} in junctional SR and corbular SR was significantly higher than ΣCa_{myo}; this difference disappeared during early systole and reappeared during late systole. Quantitatively, however, the decrease in ΣCa_{SR} cannot account for the increment in ΣCa_{myo}. The amount of released calcium is 46 μmol (the product of the decrease of ΣCa_{SR}, 1300 μM, and the volume fraction of the SR, 3·5 %). This contrasts with 428 μmol calcium necessary to increment ΣCa_{myo} by 750 μM (obtained by multiplication with 57 % myofibrillar space). This difference could suggest that the SR is not the only source for Ca^{2+} release. We think, however, that there is not yet sufficient information for such a quantitative comparison and its conclusion. For the guinea-pig ventricular myocyte, the volume fraction of the SR is yet not known, and it is not certain whether Ca^{2+} is released from the junctional SR only or also from free and peripheral SR (close to the surface membrane). Also, EPMA most probably underestimated ΣCa_{SR}. Since the diameter of the junctional SR and free SR (40 nm) is smaller than the thickness of the cryosection (120 nm), the concentrations ΣCa_{SR} are smeared by inclusion of portions of adjacent myoplasm. Up to now, no results have been published that tackle this problem for cardiac preparations in an acceptable way.

Calcium redistribution

The systolic increment of 750 μM ΣCa_{myo} raises the question whether the SR Ca^{2+}-ATPase is powerful enough for its rapid reduction during the cardiac cycle, i.e. whether the biochemical data about the SR Ca^{2+}-ATPase were compatible with the removal of 750 μM ΣCa_{myo} within about 100 ms. According to Hasselbach & Oetliker (1983), cardiac SR vesicles pump 2 micromoles calcium per milligram protein and per minute. Assuming 3 mg pump protein per millilitre wet weight cardiac tissue, and a correction factor of 5 for the difference between 20 and 36 °C, this SR ATPase activity would reduce ΣCa_{myo} from 1400 to 650 μM within about 0·7 s. The comparison with Fig. 9 shows that ΣCa_{myo} falls within about 0·1 s. The difference could have resulted from an activity loss during the biochemical isolation steps. Alternatively, one could postulate additional structures removing Ca^{2+} and releasing it again during the early systole.

The active transport of 750 μM ΣCa_{myo} into the SR requires energy in form of ATP. In cardiac SR, transport of 1 mole calcium couples to the split of 1 mole ATP. Since 1 mole ATP bears 46 kJ, transport of 750 μM ΣCa_{myo} from the myofibrillar space into the SR should correspond to an energy equivalent of 41 J. For the egress of 0·8 mM-mitochondrial calcium an additional 5·8 J (l cells)$^{-1}$ would be required (Gunter & Pfeiffer (1990). Measurements of O_2 consumption (e.g. Bünger & Permanetter, 1984) and calorimetric studies (Daut & Elzinga, 1988) suggest for the working guinea-pig myocardium a heat production of 59–69 mV (g tissue wet weight)$^{-1}$ which can be translated to 120 V (l intracellular space)$^{-1}$. Thus, in the potentiated cell, calcium shifts during the cardiac cycle may consume about one-third of the total energy.

This work was supported by the Deutsche Forschungsgemeinschaft We 879/3–2 and Is 24/7–2.

REFERENCES

ALLEN, D. G., EISNER, D. A., PIROLO, J. S. & SMITH, G. L. (1985). The relationship between intracellular calcium and contraction in calcium-overloaded ferret papillary muscles. *Journal of Physiology* **364**, 169–182.

ALLEN, D. G. & KURIHARA, S. (1980). Calcium transients in mammalian ventricular muscle. *European Heart Journal* **1**, suppl. A, 5–12.

BAYLOR, S. M. & HOLLINGWORTH, S. (1988). Fura-2 calcium transients in frog skeletal muscle fibres. *Journal of Physiology* **403**, 151–192.

BECKER, P. L., WALSH, J. V., SINGER, J. J. & FAY, F. S. (1988). Calcium buffering capacity, calcium currents and $[Ca^{2+}]_i$ changes in voltage-clamped, fura-2 loaded single smooth muscle cells. *Biophysical Journal* **53**, 595a.

BENDUKIDZE, Z., ISENBERG, G. & KLÖCKNER, U. (1985). Ca-tolerant guinea-pig ventricular myocytes as isolated in the presence of 250 μM free calcium. *Basic Research of Cardiology* **80**, 13–18.

BEUCKELMANN, D. J. & WIER, W. G. (1988). Mechanism of release of calcium from sarcoplasmic reticulum of guinea-pig cardiac cells. *Journal of Physiology* **405**, 233–255.

BLATTER, L. A. & MCGUIGAN, J. A. S. (1986). Free intracellular magnesium concentration in ferret ventricular muscle measured with ion selective micro-electrodes. *Quarterly Journal of Experimental Physiology* **71**, 467–473.

BLINKS, J. R. & ENDOH, M. (1986). Modification of myofibrillar responsiveness to Ca^{++} as an inotropic mechanism. *Circulation* **73**, suppl. III, 85–98.

BOND, M., JARAKI, A. R., DISCH, C. H. & HEALY, B. P. (1989). Subcellular calcium content in cardiomyopathic hamster hearts *in vivo*: an electron probe study. *Circulation Research* **64**, 1001–1012.

BÜNGER, R. & PERMANETTER, B. (1984). Parallel stimulation of inotropism and pyruvate dehydrogenase in perfused heart. *American Journal of Physiology* **247**, C45–52.

CALLEWAERT, G., CLEEMANN, L. & MORAD, M. (1988). Epinephrine enhances Ca^{2+} current-regulated Ca^{2+} release and Ca^{2+} reuptake in rat ventricular myocytes. *Proceedings of the National Academy of Sciences of the USA* **85**, 2009–2013.

CROMPTON, M., MOSER, R., LÜDI, H. & CARAFOLI, E. (1978). The interrelations between the transport of sodium and calcium in mitochondria of various mammalian tissues. *European Journal of Biochemistry* **82**, 25–31.

DAUT, J. & ELZINGA, G. (1988). Heat production of quiescent ventricular trabeculae isolated from guinea-pig heart. *Journal of Physiology* **398**, 259–275.

DUBELL, W. H. & HOUSER, S. R. (1989). Voltage and beat dependence of Ca^{2+} transient in feline ventricular myocytes. *American Journal of Physiology* **257**, H746–759.

FABIATO, A. (1983). Calcium-induced release of calcium from the cardiac sarcoplasmic reticulum. *American Journal of Physiology* **245**, C1–14.

FRY, C. H., HARDING, D. P. & MILLER, D. J. (1989). Non-mitochondrial ion regulation in rat ventricular myocytes. *Proceedings of the Royal Society* B **236**, 53–77.

FRY, C. H., POWELL, T., TWIST, V. W. & WARD, J. P. T. (1984). Net calcium exchange in adult rat ventricular myocytes: an assessment of mitochondrial calcium accumulation capacity. *Proceedings of the Royal Society* B **223**, 223–238.

GANITKEVICH, V. YA. & ISENBERG, G. (1991). Depolarization-mediated intracellular calcium transients in isolated smooth muscle cells of the guinea-pig urinary bladder. *Journal of Physiology* **435**, 187–205.

GRYNKIEWICZ, G., POENIE, M. & TSIEN, R. W. (1985). A new generation of Ca^{2+} indicators with greatly improved fluorescent properties. *Journal of Biological Chemistry* **260**, 3440–3450.

GUNTER, T. E. & PFEIFFER, D. R. (1990). Mechanism by which mitochondria transport calcium. *American Journal of Physiology* **258**, C755–786.

HALL, T. A. (1979). Biological X-ray microanalysis. *Journal of Microscopy* **117**, 145–163.

HASSELBACH, W. & OETLIKER, H. (1983). Energetics and electrogenicity of the sarcoplasmic reticulum calcium pump. *Annual Reviews of Physiology* **45**, 325–339.

HUXLEY, H. E. & FARUQI, A. R. (1983). Time-resolved X-ray diffraction studies on vertebrate striated muscle. *Annual Reviews Biophysical Bioengineering* **12**, 381–417.

ISENBERG, G. (1982). Ca entry and contraction as studied in isolated bovine ventricular myocytes. *Zeitschrift für Naturforschung* **37c**, 502–512.

ISENBERG, G. & WENDT-GALLITELLI, M. F. (1990). X-ray microprobe analysis of sodium concentration reveals large transverse gradients from the sarcolemma to the centre of voltage-clamped guinea-pig ventricular cells. *Journal of Physiology* **420**, 86*P*.

JOERGENSEN, A. O., BRODERICK, R., SOMLYO, A. P. & SOMLYO, A. V. (1988). Two structurally distinct calcium storage sites in rat sarcoplasmic reticulum: an electron microprobe analysis study. *Circulation Research* **63**, 1060–1069.

KITAZAWA, T., SHUMAN, H. & SOMLYO, A. P. (1983). Quantitative electron probe analysis: problems and solutions. *Ultramicroscopy* **11**, 251–262.

KRAUSE, E. G., BARTEL, S., AMELIN, I., BEYERDÖRFER, I., FREIER, W. & REESE, D. (1987). Transient activation of cyclic AMP-dependent protein kinase and phosphorylase during the cardiac cycle in the canine myocardium in situ and the effect of propranolol. *Biomedica Biochimica Acta* **46**, 482–486.

LEE, H.-C. & CLUSIN, W. T. (1987). Cytosolic calcium staircase in cultured myocardial cells. *Circulation Research* **61**, 934–939.

LEWARTOWSKI, B. & PYTKOWSKI, B. (1987). On the subcellular localization of calcium fraction correlating with contractile force of guinea-pig ventricular myocardium. *Biomedica Biochimica Acta* **46**, S345–350.

MCCORMACK, J. G., HALESTRAP, A. P. & DENTON, R. M. (1990). Role of calcium ions in regulation of mammalian intramitochondrial metabolism. *Physiological Reviews* **70**, 391–425.

MCMILLIN-WOOD, J., WOLKOWICZ, P. W., CHU, A., TATE, C. A., GOLDSTONE, M. A. & ENTMAN, M. L. (1980). Calcium uptake by two preparations of mitochondria from heart. *Biochimica et Biophysica Acta* **591**, 251–265.

NICCHITTA, C. V. & WILLIAMSON, J. R. (1984). Spermin. A regulator of mitochondrial calcium cycling. *Journal of Biological Chemistry* **259**, 12978–12983.

PAGE, E. (1978). Quantiative ultrastructural analysis in cardiac membrane physiology. *American Journal of Physiology* **235**, C147–158.

PAN, B. S. & SOLARO, R. J. (1987). Calcium-binding properties of troponin C in detergent-skinned heart muscle fibers. *Journal of Biological Chemistry* **262**, 7839–7849.

PERSSON, L. & ROSENGREN, E. (1983). Polyamine metabolism in muscles of mice and rats. *Acta Physiologica Scandinavica* **117**, 457–460.

POLIMENI, P. I. (1974). Extracellular space and ionic distribution in rat ventricle. *American Journal of Physiology* **227**, 676–683.

ROBERTSON, S. P., JOHNSON, J. D. & POTTER, J. D. (1981). The time-course of Ca^{2+} exchange with calmodulin, troponin, parvalbumin, and myosin in response to transient increase in Ca^{2+}. *Biophysical Journal* **34**, 559–569.

SHEPHERD, N., VORNANEN, M. & ISENBERG, G. (1990). Force measurements from voltage-clamped guinea pig ventricular myocytes. *American Journal of Physiology* **258**, H452–459.

SOLARO, R. J., WISE, R. M., SHINER, J. S. & BRIGGS, F. N. (1974). Calcium requirements for cardiac myofibrillar activation. *Circulation Research* **34**, 525–530.

SOMLYO, A. P., BOND, M. & SOMLYO, A. V. (1985). Calcium content of mitochondria and endoplasmic reticulum in liver frozen rapidly *in vivo*. *Nature* **314**, 622–625.

SOMLYO, A. V., GONZALES-SERRATOS, H., SHUMAN, H., MCCLENNAN, G. & SOMLYO, A. P. (1981). Calcium release and ionic changes in the sarcoplasmic reticulum of tetanized muscle: an electron-probe study. *Journal of Cell Biology* **90**, 577–594.

WENDT-GALLITELLI, M. F. (1985). Presystolic calcium-loading of the sarcoplasmic reticulum influences time to peak force of contraction. X-ray microanalysis of rapidly frozen guinea-pig ventricular muscle preparations. *Basic Research of Cardiology* **80**, 617–625.

WENDT-GALLITELLI, M. F. (1986). Ca pools involved in the regulation of cardiac contraction under positive inotropy. X-Ray microanalysis of rapidly frozen ventricular muscles of the guinea-pig. *Basic Research of Cardiology* **81**, suppl. 1, 25–32.

WENDT-GALLITELLI, M. F. & ISENBERG, G. (1989). X-ray microanalysis of single cardiac myocytes frozen under voltage-clamp conditions. *American Journal of Physiology* **256**, H574–583.

WENDT-GALLITELLI, M. F. & ISENBERG, G. (1990). Time course of myofibrillar calcium during the cardiac cycle. X-Ray microprobe analysis of voltage-clamped guinea-pig ventricular myocytes. *Journal of Physiology* **429**, 15*P*.

WENDT-GALLITELLI, M. F., JACOB, R. & WOLBURG, H. (1982). Intracellular membranes as boundaries for ionic distribution. In situ elemental distribution in guinea pig heart muscle in different defined electromechanical coupling states. *Zeitschrift für Naturforschung* **37C**, 712–720.

WERKHEISER, W. C. & BARTLEY, W. (1957). The study of steady-state concentrations of internal solutes of mitochondria by rapid centrifugal transfer to a fixation medium. *Biochemical Journal* **66**, 79–91.

WHEELER-CLARK, E. S. & TORMEY, J. MCD. (1987). Electron probe x-ray microanalysis of sarcolemma and junctional sarcoplasmic reticulum in rabbit papillary muscles: low sodium-induced calcium alterations. *Circulation Research* **60**, 246–252.